Geomorphology, 4 (1991) 161–186
Elsevier Science Publishers B.V., Amsterdam

Multivariate characterization of meandering

Alan D. Howard[a] and Allen T. Hemberger[b]
[a]*Department of Environmental Sciences, University of Virginia, Charlottesville, VA 22903, USA*
[b]*490 Huron Ave., Cambridge, MA 02138, USA*

(Received February 25, 1991; accepted after revision July 12, 1991)

ABSTRACT

Howard, A.D. and Hemberger, A.T., 1991. Multivariate characterization of meandering. *Geomorphology*, 4: 161–186.

A suite of 40 morphometric variables has been measured on 57 sections of freely meandering channels from 33 rivers. These objective variables are computed from digitized traces of the channel centerline and include measures of sinuosity, meander wavelength, curvature moments, meander asymmetry, and pattern irregularity. Several variables are measured on the half-meanders defined by successive inflection points. Principal components analysis reveals that morphological variations between freely meandering streams can be resolved into four factors related to meander wavelength, meander irregularity, sinuosity, and large-scale wandering of the meander axis. Discriminant analysis using the morphometric variables results in almost perfect separation between natural streams and two theoretical models of meander planform (Ferguson's disturbed periodic model and Howard and Knutson's simulation model), despite visual similarities. The simulated meanders are too regular in size and shape in relation to natural ones, perhaps because the interaction of effects of curvature and alternate bars upon topography and flow structure in natural channel bends produces multiple scales of bank erosion not accounted for in present simulation models.

Introduction

The meandering pattern that characterizes many streams is nearly, or "quasi-" periodic in direction or curvature such that there is a characteristic scale of meandering albeit with much irregularity in detail (Ferguson, 1976, 1979). The richness of the meandering pattern has previously been measured by only a few variables, such as wavelength, amplitude, bend radius of curvature, and sinuosity, which provide a partial, and often subjectively measured characterization. Although strong and consistent relationships exist between such variables (e.g., Leopold and Wolman, 1957, 1960; Schumm, 1968; Hey, 1976, 1984; Williams, 1986), a more complete description of meandering patterns is needed in order to compare streams, to relate differences in pattern to controlling environmental parameters, and to test the applicability of theoretical models of meandering, such as the disturbed periodic model of Ferguson (1976, 1979) (abbreviated DPM) and the simulation model of Howard and Knutson (1984) (abbreviated HKM). For example, Fig. 1 shows portions of the Red River, Minnesota and a comparative HKM simulation. The figure also shows the Smoky Hill River, Kansas compared to a DPM stream. These channel patterns are similar in wavelength and sinuosity, as well as in degree of irregularity, but subtle differences between the patterns exist that traditional measures of meander pattern cannot detect.

Several new variables are introduced in this paper that can be measured objectively from digitized centerline traces of meandering channels and automatically calculated by computer analysis. A number of issues related to the collection and analysis of data from natu-

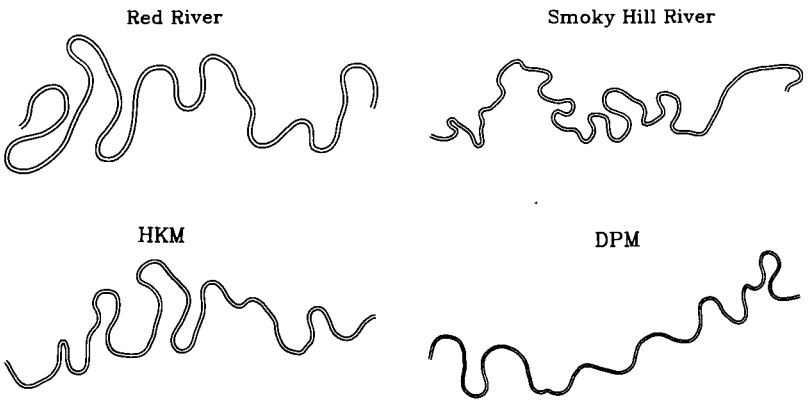

Fig. 1. Representative channel patterns for natural and simulated meandering streams. Each trace shows a length of 300 width-equivalents. The natural stream traces have been digitized, smoothed and portrayed with a uniform width equal to their average width.

ral streams are also considered, including (1) procedures for digitizing that maximize fidelity, (2) optimal sampling step length along the channel, (3) the total length of channel that should be sampled to adequately characterize the meandering pattern, and (4) objective procedures for recognition of statistical nonconstancy of meandering pattern in a downstream direction (for example, increased discharge from tributaries can increase the dominant wavelength of meandering).

These new variables, together with some traditional statistics of meandering, were measured on 57 sections of freely meandering channels from 33 rivers. This multivariate database was examined by principal component analysis to determine the principal modes by which meandering channels differ from one another. A similar, but independent multivariate approach has been developed by M.J. O'Neill (1987).

Finally, the database of natural streams is compared by discriminant analysis with a sample of centerlines generated by two theoretical models, Ferguson's DPM (1976, 1979) and the Howard and Knutson (1984) HKM. The multivariate statistical variables permit nearly perfect discrimination between the natural streams (abbreviated NAT) and the two models, despite the apparent visual similarities of the patterns. Several explanations for the shortcomings of the HKM and DPM model are discussed.

Statistical variables

The variables that have been defined for this study were created to measure a wide variety of channel pattern characteristics (see Appendix). The major constraint in their definition was that they could be objectively measured by computer from digitized centerline traces. The subjective nature of many previous studies of meander geometry, as well as the need for objective procedures, was emphasized by Hooke (1984) and O'Neill and Abrahams (1986). The statistical variables were also designed so that they could be analyzed by a single pass through the digitized coordinates without storing of individual points, so that long traces could be examined without exhausting computer memory.

The present study defines a variety of morphometric variables, several of which are strongly related (correlated) to each other while not being mathematically identical. Thus the suite of variables is partly redundant. However, the variables are readily measured by computer so that the a priori elimination of closely related variables does not save appre-

ciable labor or computer resources. Furthermore, the degree of redundancy is not generally known in advance, and subtle aspects of meander shape may be revealed by the non-correlative components of otherwise strongly related variables. The topic of variable redundancy is considered again later.

The variables can be roughly grouped into two categories, those that are *ensemble* averages for the entire measured channel, and *half-meander* statistics measured on individual portions of channel between successive inflection points, or crossings. The ensemble statistics include measures of sinuosity, spectral characteristics, and estimated autoregressive parameters. The half-meander statistics describe the shape and size of individual half-meanders, and are summarized as averages by categories of size of meander.

Ensemble statistics

Ensemble statistics are calculated as statistical moments or total values of a variable for the entire sampled stream path. These fall into four classes discussed below.

Measures of sinuosity. Total sinuosity, μ_T, was one of the first variables to be measured on meandering streams, and is defined as the total pathlength divided by the straight-line distance, D, between the initial and final points of the measured stream path:

$$\mu_T = \sum_{i=1}^{n} l_i / D \tag{1}$$

where the l_i are the individual digitized stream segment lengths. Three non-traditional measures of sinuosity have been defined (Fig. 2). All are based upon subdividing the stream into individual half-meanders, which are defined as segments of stream lying between successive inflection points (locations where the channel curvature changes sign downstream). The new measures of sinuosity are the full-meander sinuosity, μ_W, the half-meander sinuosity, μ_H, and the residual sinuosity, μ_R:

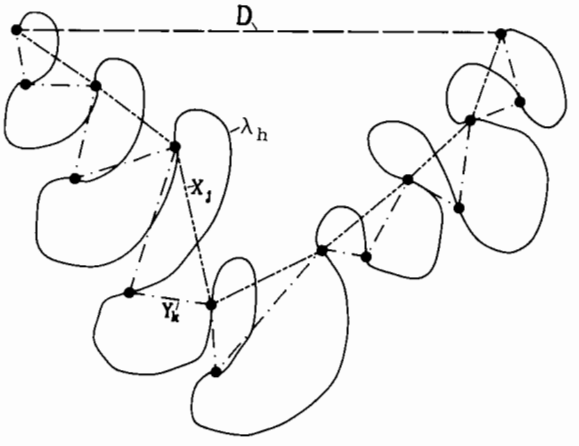

Fig. 2. A hypothetical channel centerline (solid line) showing location of inflection points (solid dots) and the straight-line (long dashes), whole-meander (long and short dashes), and half-meander paths (dash–dots). The symbols are the lengths of the paths between the defining inflection points.

$$\mu_R = \sum_{j=1}^{l} X_j / D \tag{2}$$

$$\mu_W = \sum_{k=1}^{m} Y_k / \sum_{j=1}^{l} X_j \tag{3}$$

$$\mu_H = \sum_{i=1}^{n} l_i / \sum_{k=1}^{m} Y_k \tag{4}$$

The full-meander pathlength is defined as the summation of the lengths, X_j, of the straight-line paths connecting every other inflection point, i.e., inflection points defining one wavelength of meandering. Similarly, the half-meander pathlength sums the lengths, Y_k, of the straight-line paths connection successive inflection points. If an odd number of inflection points is sampled, then the total number of half-meanders, m, will be twice the number, l, of full-meanders. Note that the total sinuosity is the product of the other sinuosities:

$$\mu_T = \mu_W \mu_H \mu_R \tag{5}$$

Many natural streams exhibit pronounced wanderings of the valley axis due to topo-

graphic and structural controls. This wandering becomes incorporated into the residual sinuosity. To provide an estimate of the structural component of the total sinuosity, a valley sinuosity, μ_V, is defined by averaging the x and y coordinate values of successive groups of 100 consecutive digitized points (longer than the characteristic scales of meandering since the distance between digitized points is about one channel-width equivalent). The sinuosity of these averaged locations is the valley sinuosity.

The whole-meander sinuosity would be unity for a regular, symmetrical meandering path, but is greater than one for regular, but asymmetrical meander loops, such as those shown in Fig. 2, or for meander paths with irregular, or "random" components. The half-meander sinuosity measures the amplitude of half-meanders relative to their length.

Spectral variables. Speight (1965, 1967) pioneered the use of spectral analysis to characterize river meandering, with subsequent contributions by Chang and Toebes (1970), Thakur and Scheidegger (1968, 1970) and Ferguson (1975). Although the spectrum of direction or curvature contains a wealth of quantitative information about the wavelengths of meandering, the use of the spectrum has largely been qualitative, with interpretation limited to characterization of the meandering as being regular (one dominant wavelength), irregular (a wide range of wavelengths with no dominant peak), or multimodal. The exception has been the suggestion by Ferguson (1975) to use the direction and curvature spectra to estimate the dominant wavelength.

It is commonly asserted that the meander spectrum fully characterizes the meander pattern (e.g., O'Neill and Abrahams, 1986, p. 338). However, the spectrum is a statistical summary representing N original data points (curvature or direction) by a smaller number, K, of frequency estimates. Much information about ordering of individual data points is not represented in the spectrum, and the spectrum is only meaningful for stationary processes (in the analysis of time series, temporal constancy of the statistical properties of the time series is termed *stationarity*; in the case of meandering, we are concerned with spatial constancy and the series is the meander planform).

The curvature spectrum was utilized in the present study because the direction spectrum is strongly affected by large wanderings of the valley centerline and because the peak in the curvature spectrum is a measure of the dominant wavelength of meandering (Ferguson, 1976). Theoretical models of stream meandering (Ikeda et al., 1981; Howard and Knutson, 1984) suggest that the erosion of channel banks creating meandering is controlled by the effects of the downstream pattern of channel curvature upon near-bank velocities. Similarly, Ferguson's DPM can be characterized by its curvature spectrum.

Three variables were measured from the curvature spectrum. The first is the peak wavelength of meandering, λ_P, defined by the wavelength associated with the highest spectral variance. The second is the average wavelength of meandering, $\lambda_{\{av\}}$, defined as two pi times the reciprocal of the average frequency:

$$\lambda_{\{av\}} = 2\pi / \left(\sum_{i=1}^{n} v_i k_i / \sum_{i=1}^{n} v_i \right) \qquad (6)$$

where v_i is the spectral variance associated with the frequency k_i, and the summation is taken over the range of frequencies estimated by the spectral analysis. Because the spectra of river meandering are dominated by low-frequency components and is thus strongly skewed, the average wavelength is shorter than the dominant wavelength. Finally, a coefficient of variation of the frequency, $k_{\{cv\}}$, is defined as the standard deviation of the frequency divided by the average frequency. Because the spectral wavelength estimates are based upon following the path of the stream rather than a down-valley axis, spectral wavelengths (as well as the other types of wavelength estimates used in this

study) will be larger than the traditional downvalley wavelength estimates by a factor equal to the total sinuosity.

Some meander spectra exhibit two or more distinct peaks in their spectrum. However, no convenient and continuous measure of multi-peakedness was devised. Multi-peaked spectra tend to be associated with high values of the ratio of dominant to average wavelength and a large standard error of the frequency. However, widely dispersed, but weakly single-peaked spectra share these characteristics.

Autoregressive parameters. Ferguson (1975, 1976, 1979) suggested that stream meandering can be closely approximated by a DPM:

$$\theta+\frac{2d}{k}\frac{\mathrm{d}\theta}{\mathrm{d}s}+\frac{1}{k^2}\frac{\mathrm{d}^2\theta}{\mathrm{d}s^2}=e \tag{7}$$

where θ is the direction angle of the stream centerline (arbitrary reference), s is distance following the stream centerline, k is the dominant frequency of meandering, d is a damping factor, and e is a random forcing assumed to be normal Gaussian white noise. This is equivalent to a second-order autoregressive model (Box and Jenkins, 1976) in which:

$$\theta_i=C_1\theta_{i-1}+C_2\theta_{i-2}+E_i \tag{8}$$

where C_1 and C_2 are parameters, E_i is an error, or disturbance, term (also Gaussian white noise), the present value of direction is θ_i, and θ_{i-1} and θ_{i-2} are the values of θ at equally-spaced past steps. If symmetrical difference approximations are used for the derivatives in eq. (7), then the parameters in the autoregressive model are estimated as follows:

$$C_1=(2-k^2s^2)/(ksd+1) \tag{9}$$

$$C_2=(ksd-1)/(ksd+1) \tag{10}$$

$$E=ek^2s^2/(ksd+1) \tag{11}$$

where s is the path length of successive steps. An instrumental variable approach was used to estimate C_1, C_2, and the variance of E from equally-spaced digitized centerline data using a modified version of the CAPTAIN program (Young, 1984). Then eqns. (9–11) are solved for equivalent estimated values of d, k, and e. This estimating procedure was used both on the directional and curvature time series for the digitized stream, yielding a total of six estimates, d_θ, k_θ, e_θ, d_ξ, k_ξ, and e_ξ, where θ refers to the directional and ξ to the curvature estimates. The values for the frequencies are entered into the database as their equivalent wavelengths, λ_θ and λ_ξ. Also, the error values used in the database, e'_θ and e'_ξ, have been normalized by the frequency and step length:

$$e'=\frac{e}{ks} \tag{12}$$

Ferguson (1979) presents asymptotic expressions for the autoregressive parameters C_1 and C_2, and Box and Jenkins (1970) similarly present asymptotic estimates for d and k. However, the estimate of k fails if the estimated values of C_1 and C_2 are such that the process is unstable ($d>1$). For many natural streams the estimated parameters are such that the second-order autoregressive process is unstable. However, the discrete estimates for d and k given above provide reasonable values for k even when $d>1$.

The autoregressive parameters C_1 and C_2 are also used to detect certain forms of non-stationarity in the digitized centerlines, as discussed further below.

Summary curvature statistics. The frequency distribution of curvature or its inverse, the radius of curvature, have sometimes been used to characterize meander patterns. Curvature or wavelength is generally normalized by the average channel width, W, so that normalized curvature, ξ, is defined as:

$$\xi=W\frac{\mathrm{d}\theta}{\mathrm{d}s} \tag{13}$$

and is estimated by:

$$\xi=2W\theta/(l_i+l_{i+1}) \tag{14}$$

where l_i and l_{i+1} are the lengths of successive digitized stream segments and θ is the change in direction angle between the two segments (a clockwise θ is positive). The channel width used in this study is an average of many repeated measurements made from the topographic maps from which the centerline was digitized. As such, the width used to normalize these and other variables is generally somewhat smaller than the bankfull value used in other studies.

A curvature value is calculated for each sample step along the meander path, and the first four statistical moments are calculated for both the raw, or signed, curvature values (which are positive in meanders curving clockwise downstream) and for the absolute curvature values, $|\xi|$. The first moment is represented as the average curvature, $\xi_{\{av\}}$, the second as the standard deviation, $\xi_{\{sd\}}$, the third as the skewness, $\xi_{\{sk\}}$, where skewness is defined as:

$$\{sk\} = M_3/(M_2)^{1.5} \tag{15}$$

and M_N is the Nth statistical moment:

$$M_N = \sum_{i=1}^{n} (x_i - \bar{X})^N/(n-1) \tag{16}$$

and x_i are the individual data points and $\bar{X}$ is the sample mean. Similarly, the curvature kurtosis, $\xi_{\{kr\}}$, is based on the definition:

$$\{kr\} = (M_4/M_2^2). \tag{17}$$

In some analyses the standard deviation is replaced by the coefficient of variation, $\{cv\}$.

Because left- and right-handed half-meanders are generally statistically similar, the average and skewness of raw curvature are very close to zero and not included in the database, but these moments are retained for the absolute curvatures, giving the moments $|\xi|_{\{av\}}$, $|\xi|_{\{sd\}}$, $|\xi|_{\{sk\}}$, and $|\xi|_{\{kr\}}$.

The above moments were also calculated for three other variables. The first is the half-meander curvature, ξ_H, defined as:

$$\xi_H = 2W\varphi_k/(Y_k + Y_{k+1}) \tag{18}$$

where φ_k is the absolute value of the direction angle between the lines connecting successive inflection points of individual half-meanders. The full-meander curvature, ξ_W, is defined analogously:

$$\xi_W = 2W\psi_j/(X_j + X_{j+1}) \tag{19}$$

Finally, summary statistical moments were calculated for the half-meander wavelengths, λ_{hk}, where λ_h is defined as the width-normalized pathlength measured along the centerline between successive inflection points.

Half-meander statistics

A meandering stream consists of sections of alternating sign of curvature, with inflection points, crossings, or endpoints at the points of zero curvature. O'Neill and Abrahams (1986) call the individual sections having the same sense of curvature "half-meander", while Howard (1983) called then "half-loops". The half-meander terminology is used here. Two successive half-meanders constitute a full-meander. The half- and full-meanders are the fundamental building blocks of a meandering stream, so that statistical characterization of their shape and size is desirable.

O'Neill and Abrahams (1986) point out that determination of inflection points is the crucial step in identification of half-meanders, and that different procedures will yield different numbers of inflection points. Small irregularities in direction, or in some cases small-scale meandering superimposed upon larger meanders, are present in the planform of natural streams. Therefore, the number of identified half-meanders depends upon the sample interval along the meander path, decreasing as the resolution coarsens. Furthermore, errors in determining the centerline or in digitizing the centerline introduce unintended inflection points. The short half-meanders created by the real and introduced small regularities can dominate over longer, more sinuous half-meanders. O'Neill and Abrahams (1986, p.

338) feel that long half-meanders characterize the meandering pattern more fully than the short ones, distinguishing between "insignificant curves in a channel and true half-meanders". Consequently, they introduce a minimum total direction change, or "half-meander tolerance", that distinguish "simple" half-meanders from straight reaches. Two or more simple half-meanders with the same sense of curvature (together with the intervening straight sections) constitute a "complex" half-meander.

A different approach is taken here, based upon the assumption that both the large and small bends convey important information about the meander pattern. Each inflection point defined by downstream change of sign of the digitized curvatures is taken to define a new half-meander, which is characterized by several statistical measures. However, the initial sampling procedure, discussed below, includes a certain degree of averaging so as to minimize introduction of inflection points due to digitizing errors. This averaging, of course, filters out certain true inflection points for half-meanders shorter in length than the equivalent of about one to two channel widths. Nonetheless, as will be discussed below, this procedure, when applied consistently, gives a reasonable characterization of half-meander sizes and shapes.

Several measures of size and shape of half-meanders have been defined, some of which were suggested by Howard (1983). The first of these is the wavelength of the half-meander, λ_h, measured along the channel centerline (λ_h is measured on individual half-meanders, whereas the ensemble statistics, $\lambda_{h\{av\}}$ etc., are measured for all half-meanders taken together). This length is used to separate half-meanders into classes of width-normalized length. In this study, the classes ranged from one to sixty width-units. The total number of half-meanders and the average value of each of the variables defined below were determined for each length class.

The second half-meander variable is the sinuosity, μ_h:

$$\mu_h = \lambda_h / Y_h \tag{20}$$

where Y_h is the straight-line distance between the inflection points defining the half-meander. The average absolute curvature, $|\xi|_{h\{av\}}$, is defined as:

$$|\xi|_{h\{av\}} = \sum_{i=1}^{n} |\xi|_i / n \tag{21}$$

where n is the total number of digitized points within the half-meander. The standard deviation of curvature, $|\xi|_{h\{sd\}}$, is defined analogously. The curvature ratio, $R_{\xi h}$, is the ratio of the maximum curvature, $|\xi|_{h\{max\}}$, to the average curvature:

$$R_{\xi h} = |\xi|_{h\{max\}} / |\xi|_{h\{av\}} \tag{22}$$

A length-normalized dimensionless curvature, $|\xi|_{h\lambda}$, is defined (after Ferguson, 1973) as the product of the average curvature times the meander wavelength divided by the channel width:

$$|\xi|_{h\lambda} = |\xi|_{h\{av\}} \lambda_h / W \tag{23}$$

Thus $|\xi|_{h\lambda}$ is curvature-normalized by the half-meander length rather than by channel width.

The tendency of meanders to be asymmetrical, generally with the sharpest curvatures near the upstream end of the meander, has been noted by Brice (1974a), Nanson (1980), Davies and Tinker (1984), Howard and Knutson (1984), Lapointe and Carson (1986) and measured by Carson and Lapointe (1983). Their technique, based upon definition of a valley axis, is not well suited to the procedures used in the present study. Two alternative measures based upon the half-meander have been defined. The simplest is based upon definition of the locus of maximum curvature in the bend. This breaks the half-meander into two segments, upstream and downstream, of length λ_u and λ_d (Fig. 3A). The asymmetry index 1, $\mathcal{A}_{h1}$, is defined as:

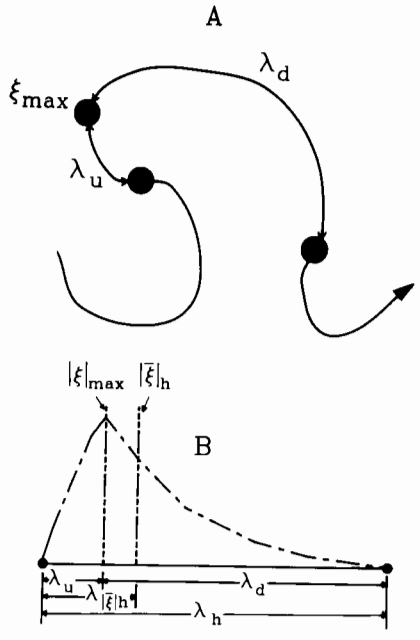

Fig. 3. Definition of half-meander variables for asymmetry variables. $|\xi|_{max}$ is locus of maximum curvature on half-meander (solid dot in A), and λ_μ and λ_d are the path lengths of the channel centerline above and below $|\xi|_{max}$. Long and short dashed line in B is the curvature as a function of position along the centerline, and $\lambda_{|\xi|h}$ is the locus of the average curvature.

$$\mathscr{A}_{h1} = (\lambda_u - \lambda_d)/\lambda_h \tag{24}$$

which has values between +1 and −1, with negative values for a maximum lying upstream of the center of the half-meander path. A second asymmetry index is based upon finding the locus of mean curvature, $\lambda_{|\xi|h}$, along the half-meander path (Fig. 3B):

$$\lambda_{|\xi|h} = \sum_{i=1}^{n} s_i |\xi|_i / \sum_{i=1}^{n} s_i \tag{25}$$

where the s_i are the distances along the centerline from the beginning of the half-meander to the location of each measured absolute curvature. The second asymmetry index, $\mathscr{A}_{h2}$, is defined as:

$$\mathscr{A}_{h2} = (2\lambda_{|\xi|h} - \lambda_h)/\lambda_h \tag{26}$$

and it likewise varies from +1 to −1. This second index should be less sensitive to sample noise than the first index because it is based upon the curvature distribution rather than a single curvature value.

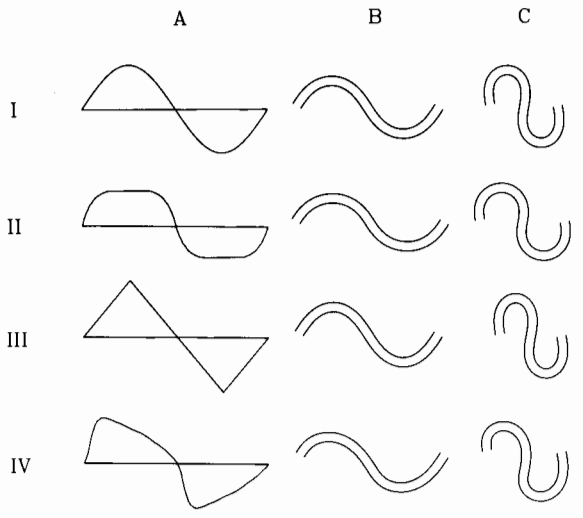

Fig. 4. Representative single meanders. Column A shows channel curvature as a function of pathlength, and columns B and C shows channel traces for different values of total sinuosity for the curvature functions in A. All channels have a wavelength of 20 width-equivalents. See Table 1 for statistical characteristics of these channels.

TABLE 1

Statistical characteristics of meander patterns shown in Fig. 4.

Variable	Channel type and variant[a]							
	IB	IC	IIB	IIC	IIIB	IIIC	IVB	IVC
μ_T	1.31	2.71	1.25	2.19	1.33	3.04	1.29	2.50
$\xi_{\{sd\}}$	0.10	0.20	0.06	0.12	0.12	0.23	0.10	0.19
$\|\xi\|_{\{av\}}$	0.2	0.35	0.2	0.35	0.2	0.35	0.2	0.35
$\|\xi\|_{h\lambda}$	2.0	3.5	2.0	3.5	2.0	3.5	2.0	3.5
$R_{\xi h}$	1.57	1.57	1.20	1.20	2.00	2.00	1.63	1.63
$\mathscr{A}_{h1}$	0.0	0.0	0.0	0.0	0.0	0.0	−0.6	−0.6
$\mathscr{A}_{h2}$	0.0	0.0	0.0	0.0	0.0	0.0	−0.16	−0.16

[a]Classification from Fig. 4.

Figure 4 shows representative meanders of various shapes and sinuosities and Table 1 summarizes their half-meander statistics.

Although the half-meander statistics are calculated for each category of width-equivalent lengths from 1 to 60, these statistics are highly variable for reasonable lengths of measured streams. Therefore the above statistics were recalculated for two length ranges of half-mean-

ders for inclusion in the database; these were the 30th through 50th percentiles of half-meander length (indicated in tables with the subscript s, for "short") and the 60th through 90th percentiles (subscript l for "long").

In addition, the number of half-meanders in seven summary length categories of 1, 2–3, 4–6, 7–10, 11–20, 21–35, and 36–60 was counted. Two ratios are defined to characterize the distribution of half-meander lengths:

$$R_m = (N_{4-6} + N_{7-10})/N_t \quad (27)$$

$$R_t = (N_1 + N_{2-3})/(N_{11-20} + N_{21-35} + N_{36-40}) \quad (28)$$

where the N values are the numbers of half-meanders in each length category, and N_t is the total number of observed half-meanders. The first ratio measures the relative number of mid-sized half-meanders, whereas the second characterizes the relative number of short to long half-meanders. Finally, the frequency distribution of half-meander wavelengths is characterized by the median half-meander length, λ_{50}, and the 90th percentile length, λ_{90}. Both are width-normalized.

Sampling procedures

Several issues are involved in collecting a sample of centerline traces from natural meandering streams, including (1) selection of streams for sampling, (2) digitizing and smoothing procedures to minimize sampling noise while retaining as much of the high frequency components of meandering as possible, (3) determining of the minimum length of stream needed for a stream sample, and (4) assuring statistical stationarity of the sampled segments.

Selection of streams

Thirty-three rivers from seventeen states are investigated. Most are midwestern or southeastern U.S. rivers. The following criteria were used in their selection:

(1) The channels were limited to those that are freely meandering, that is, with less than 15% channel impingement against valley walls or high terraces.

(2) A prospective river was rejected if there were obvious major upstream flow regulation or flow diversions within the reach. Similarly, channelization or artificial cutoffs were reasons for elimination.

(3) Individual reaches were not permitted to extend beyond major confluences.

(4) The river width had to be discernible and measurable on topographic maps.

(5) A sufficient length of channel obeying the above constraints had to be present. Sample length criteria are discussed below.

Within these limitations, the sampling was designed to provide a wide range of meander patterns, including streams of very high and very low sinuosity. Table 2 lists selected characteristics of the sampled streams. Centerline traces of the sampled streams are presented by Hemberger (1986). As is evident in Table 2, some long stream sections were broken into two or more segments either to assure a statistically stationary sample or because the initial stream segment was long enough to provide more than one sample.

Digitizing and smoothing

The representation of stream centerlines by digitizing involves important issues of noise and bias introduced by the sampling procedures. Large sampling errors were minimized by digitizing each stream in short sample sections that could be easily retraced. Despite this precaution, digitizing of the centerline unavoidably introduces small, generally high-frequency errors. Techniques to minimize these errors, such as smoothing, tend also to filter out the natural high frequency components of the sampled stream. The effect of sampling procedures upon errors was investigated by the use

TABLE 2

Summary data on streams included in database. Sample length, L, is in width equivalents, and other variables are width-normalized.

River	W (m)	L	μ_T	$\lvert\xi\rvert_{(av)}$	$\lambda_{h(av)}$	λ_θ
Arkansas, KS 1	62	897	1.19	0.109	5.3	23.2
Arkansas, KS 2	62	927	1.13	0.086	5.1	25.0
Black Fork, WY 1	33	1635	2.57	0.178	7.5	27.6
Blacks Fork, WY 2	48	897	1.96	0.218	6.3	23.0
Boulder, MT	33	599	1.32	0.140	6.8	22.7
Chena, AK	55	899	2.20	0.230	8.0	27.1
Cimarron, KS–OK	68	936	1.43	0.114	6.4	25.8
Edisto, SC	58	597	1.56	0.269	5.2	15.9
Elkhorn, NB	62	900	1.53	0.140	7.1	27.1
Fox, WI 1	36	749	1.89	0.200	5.2	22.4
Fox, WI 2	56	649	1.45	0.149	5.2	23.5
Iowa, KS	76	845	1.59	0.180	7.0	23.5
Little Pee Dee, SC 1	25	699	1.68	0.346	4.5	12.3
Little Pee Dee, SC 2	60	699	1.96	0.388	4.4	12.8
Lumber, NC–SC	40	600	1.87	0.353	5.0	15.3
Meherrin, VA–NC 1	32	847	2.10	0.262	6.4	18.6
Meherrin, VA–SC 2	32	847	2.42	0.215	6.0	22.5
Meherrin, VA–SC 3	32	856	2.01	0.184	5.9	24.6
Milk, MT 1	32	1797	2.52	0.117	10.6	49.5
Milk, MT 2	32	1797	3.51	0.106	9.4	56.8
Milk, MT 3	32	1797	3.06	0.106	10.6	61.1
Obion, TN	39	1097	1.59	0.218	5.8	34.8
Powder, MT	56	903	1.37	0.089	7.0	41.9
Red, Mn–NB 1	35	1147	1.86	0.144	8.6	32.3
Red, MN–ND 2	35	1147	2.55	0.191	8.6	32.0
Red, MN–ND 3	35	1147	2.42	0.186	7.5	28.8
Red, ND–MN 4	72	1602	2.00	0.134	10.7	38.0
Red, ND–MN 5	72	1609	1.94	0.144	8.5	36.2
Rock, IA–SD	32	1002	1.54	0.174	5.7	26.8
Rogue, MI 1	22	847	2.12	0.381	5.0	14.1
Rogue, MI 2	22	875	2.32	0.262	5.0	18.4
Saline, KS 1	24	1797	2.60	0.125	7.2	47.6
Saline, KS 2	24	1597	2.87	0.165	7.3	38.9
Saline, KS 3	24	1597	2.79	0.177	7.7	35.9
Saline, KS 4	24	1599	3.13	0.168	7.4	39.2
Saline, KS 5	24	1599	3.08	0.177	7.4	36.8
Saline, KS 6	24	1686	2.48	0.181	7.1	35.0
Savannah, SC–GA 1	106	1197	1.92	0.215	6.9	22.9
Savannah, SC–GA 2	106	1197	1.81	0.251	5.9	18.6
Sioux, IA 1	34	997	1.59	0.186	6.5	21.3
Sioux, IA 2	34	1597	2.05	0.168	5.7	25.5
Sioux, IA–SD 3	44	1197	1.84	0.178	6.7	25.5
Sioux, IA–SD 4	44	1201	2.28	0.207	7.3	22.0
Smith Fork, WY	28	697	1.71	0.351	4.7	13.9
Smoky Hill, KS 1	28	1947	2.14	0.096	7.5	50.2
Smoky Hill, KS 2	28	1947	2.51	0.121	8.4	46.2
Smoky Hill, KS 3	28	1963	3.34	0.137	8.1	43.7
Smoky Hill, KS 4	59	1497	2.11	0.177	7.6	31.9
Solomon, KS 1	26	2127	2.28	0.083	6.0	62.4
Solomon, KS 2	26	2127	2.75	0.084	7.7	68.9
Solomon, KS 3	26	2127	2.27	0.102	6.9	50.2
Solomon, KS 4	26	2131	2.58	0.124	7.0	46.9
Suwannee, GA–FL 1	38	987	1.58	0.230	6.1	17.1
Suwannee, GA–FL 2	38	987	1.74	0.128	6.6	33.0
Suwannee, GA–FL 3	38	990	1.68	0.149	6.0	27.2
Tongue, WY–MT 1	31	1194	1.75	0.203	6.9	24.8
Tongue, WY–MT 2	38	1301	2.65	0.152	7.6	38.4

of a plot of a stream generated by the DPM. The advantage of using an artificial stream trace is that the statistical characteristics of the model stream are known, so that the fidelity of digitizing procedures can be determined. The details of this study are presented by Hemberger (1986). The digitizing and sampling procedures adopted in response to this study provide an appropriate reduction of operator error while retaining most of the high-frequency information of the original stream:

(1) The centerline trace of the original stream is digitized three times, each time independently. The original density of digitized points is about 2 to 4 per width-equivalent of channel.

(2) The three files of digitized centerlines are merged into a single file that is then smoothed by an 11-point equal-weight moving average. With the 6 to 12 points per width equivalent in the merged file, the moving average has an effective length of approximately 1 to 1.5 width units.

(3) The smoothed centerline is sampled at an interval of one channel width-equivalent for statistical analysis.

(4) In order to minimize the effects of remaining sample noise upon half-meander statistics, an inflection point at a node i is recognized only if the sum of the curvatures at node i and the previous (upstream) node $i-1$ is of different sign than the sum of curvatures at i and the downstream node $i+1$ (Fig. 5). However, the curvatures are not averaged for calculation of the statistical variables. The effect

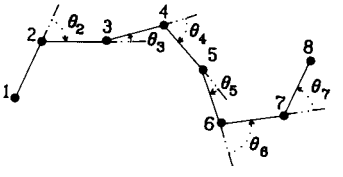

Fig. 5. Location of inflection points on digitized trace. An inflection point is not defined at node 3 because $\theta_2+\theta_3$ has the same sign as $\theta_3+\theta_4$. A similar situation occurs at node 4, but node 5 is an inflection point because $\theta_4+\theta_5$ is positive, whereas $\theta_5+\theta_6$ is negative.

of this averaging [which is similar to the O'Neill and Abrahams (1986) approach but less extreme] is to reduce the number of recognized short half-meanders of unit length, but has negligible effect on the frequency and statistical variables of longer half-meanders.

Procedures (3) and (4) are also applied to analysis of theoretical streams generated by DPM or HKM.

Minimum sample length

Many quantitative studies of meander morphometry have used measurements made on very short stream sections (including in some cases 10 or fewer full meanders). For example, Ferguson's (1979) study of meander spectra included sample lengths of 150 to 600 width-equivalents, or about 5 to perhaps 30 meander wavelengths. Unfortunately, there are no a priori criteria to determine the variability of the meander properties defined above. In order to characterize this variability, Ferguson's DPM was used to generate independent samples of meandering streams of various lengths. His model was modified to eliminate closed loops generated by the constrained random walk; such loops were eliminated by "cutoffs" and the path at the three points defining the cutoff was slightly smoothed.

Figure 6 shows plots of several of the statistical variables measured on streams of various length generated by the DPM. From these plots it is evident that statistics generated from samples of less than several tens of meander wavelengths are highly variable. Correspondingly, a minimum sample length of about 40 meanders was established, with a preferred range of 50 to 60 meanders. Very long streams were broken into subsamples within the preferred range. Because of the likelihood of non-stationarity of long segments of natural streams, it is impractical to estimate variability from digitized data. However, the DPM can be used for this purpose. Ten 50-wavelength simulated centerlines were made for a value of d, k, and e' that results in statistical characteristics close to natural meandering streams. Table 3 shows aver-

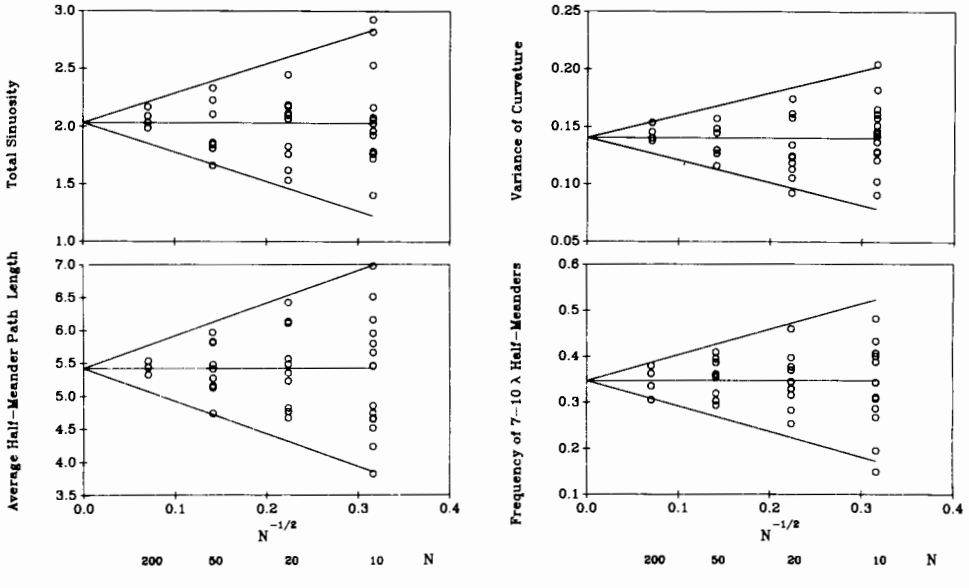

Fig. 6. Representative meander statistics for independent DPM simulated streams of different total length, N, measured in total wavelengths sampled. Ten simulations each mere made for N of 10, 20, and 50 wavelengths, and 4 for N of 200 wavelengths. The horizontal line gives the lumped average, and the slanted lines are the estimated two standard deviation envelope. See Table 3 for a summary of estimated mean and standard deviation for all measured variables for N of 50.

TABLE 3

Variability of estimated variables.

Variable	Mean value	Standard deviation
λ_θ	21.4	0.87
d_θ	0.78	0.07
e'_θ	1.02	0.044
λ_ξ	6.9	0.22
d_ξ	0.81	0.066
e'_ξ	0.48	0.02
μ_T	1.96 (0.29)	0.13 (0.030)
μ_W	1.48 (0.17)	0.086 (0.025)
μ_H	1.06 (0.025)	0.014 (0.0056)
μ_R	1.25 (0.096)	0.039 (0.013)
λ_P	18.0	3.8
$\lambda_{\{av\}}$	7.7	0.28
$k_{\{cv\}}$	0.83	0.022
$\xi_{\{sd\}}$	0.317	0.012
$\xi_{\{kr\}}$	0.33	0.41
$\lvert\xi\rvert_{\{av\}}$	0.251	0.0091
$\lvert\xi\rvert_{\{sd\}}$	0.194	0.0087
$\lvert\xi\rvert_{\{sk\}}$	1.2	0.21
$\lvert\xi\rvert_{\{kr\}}$	1.9	1.2
ξ_W	0.096	0.0096
ξ_H	0.130	0.0088
$\lambda_{h\{av\}}$	4.63	0.20
$\lambda_{h\{sd\}}$	3.18	0.17
$\lambda_{h\{sk\}}$	1.08	0.26
$\lambda_{h\{kr\}}$	1.2	1.4
μ_h	1.55 (0.19)	0.10 (0.028)
$\lvert\xi\rvert_{h\{av\}}$	0.26	0.015
$R_{\xi h}$	1.95 (0.29)	0.046 (0.010)
$\lvert\xi\rvert_{h\lambda}$	1.16	0.085
$\mathscr{A}_{h1}$	0.02	0.054
$\mathscr{A}_{h2}$	0.001	0.018
R_m	0.49 (−0.31)	0.032 (0.028)
R_l	9.4 (0.94)	3.9 (0.18)
λ_{50}	3.4	0.31
λ_{90}	8.7	0.34
$\lambda_P/\lambda_{\{av\}}$	(0.36)	(0.084)
$\lambda_{90}/\lambda_{50}$	(0.41)	(0.031
$\lambda_\theta/\lambda_\xi$	(0.48)	(0.018)
d_θ/d_ξ	(−0.02)	(0.055)
e'_θ/e'_ξ	(0.32)	(0.030)

Values are estimated from 10 simulations of 50 wavelengths of the disturbed periodic model with a wavelength of 25, $d_\theta = 0.8$, $e'_\theta = 1.2$, and 25 sample points per wavelength. Values in parentheses are equivalent values using the logarithmic transform of variables that are defined as positive ratios.

ages and standard deviations of the estimated meander variables. Most of the estimated variables have two or three significant digits, but the kurtosis measurements ($\xi_{\{kr\}}$, $|\xi|_{\{kr\}}$, and $\lambda_{h\{kr\}}$) are highly variable and the asymmetry variables ($\mathscr{A}_{h1}$, and $\mathscr{A}_{h2}$) are not statistically different from zero. The standard deviations of the estimates for natural streams or for other types of streams models may differ somewhat from the values in Table 3 and they may also be proportional to the magnitude of the estimated variable.

Sample stationarity

The meandering pattern of natural streams is affected by several factors that can change systematically downstream, including stream discharge, bed and bank sediments, and valley gradient. Although the initial screening of sample streams eliminated obvious cases of non-stationarity, objective criteria are needed to eliminate more subtle systematic downstream changes in meander pattern. To test for

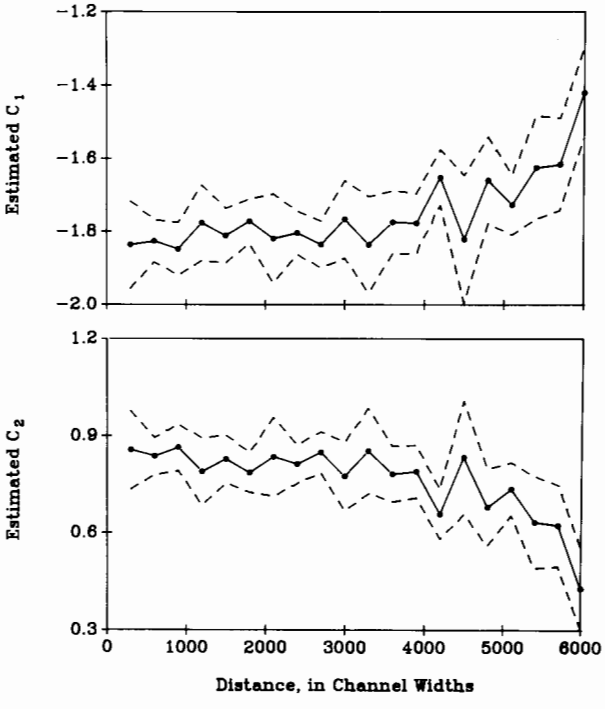

Fig. 7. Estimated values of the autoregressive parameters C_1 and C_2 (eq. 8) for the Milk River, Montana. Each point is an estimate for 300 centerline direction measurements spaced at one width equivalent distance. The dashed lines are ±2 standard deviations.

stationarity, the parameters C_1 and C_2 were estimated for the direction series of the digitized stream samples for successive series of 300 direction samples. Figure 7 shows plots of these parameters and their 90% confidence limits for the Milk River, Montana. The criterion for selection of stream segments was that all estimated values of C_1 and C_2 should lie within the 90% confidence limits of all other estimates. However, one out-of-range value of C_1 or C_2 in the middle of the series was permitted if no trend in these parameters was evident. Thus for the Milk River in Fig. 7, the portion of the channel from 0 to 3500 width-equivalents is reasonably stationary, but a trend is present for the last 1500 to 2500 width-equivalents. Although this criterion assures that the autoregressive, and probably the spectral characteristics of the sampled streams are approximately stationary, there may be other forms of non-stationarity that are not detected.

Data analysis

The statistical variables measured on the 57 natural stream segments are analyzed by two multivariate statistical techniques. The first of these is a factor analysis for the purpose of determining the basic modes of variation among meandering streams. The second technique is discriminant analysis applied to the natural streams as well as 165 streams generated by the DPM model and 227 streams simulated by the HKM model.

Factor analysis

Factor analysis (FA) is a descriptive technique for studying the correlation structure of multivariate samples, allowing interpretation of the variance-covariance structure through a few uncorrelated linear combinations, or factors, of the original set of variables (Davis, 1986; Joreskog et al., 1976; Kleinbaum and Kupper, 1978). No a priori patterns of causality are assumed. If most of the total population variance of a large variable set, m, can be attributed to the first K factors, then these can replace the original m variables without much loss of information. The objectives of FA applied to the meander data are (1) data reduction to a set of K significant factors, or "dimensions" of meandering, and (2) interpretation of the physical significance of these dimensions.

Each factor, or eigenvector, is associated with an eigenvalue giving the proportion of the total variance that is explained by that factor. A minimum eigenvalue of unity is commonly used to discriminate significant eigenvectors from apparent noise (Norusis, 1986). Better estimates of the statistical significance of eigenvectors can be obtained by comparison with analyses using data matrices composed of random variates (Preisendorfer et al., 1981; Stauffer et al., 1985). However, other concerns discussed below limit the number of physically interpretable factors to less than the number of statistically significant factors.

The relative value of the eigenvalues is a measure of the importance of the factor in the database. However, this relative ordering is not necessarily indicative of the relative importance of a corresponding "real" or "physical" factor in the target population (the meandering centerline). A lack of correspondence between the statistical model and the characteristics of the meandering centerline can arise (1) because essential elements of the natural meandering pattern have not been measured (say, for example, that no measures of half-meander asymmetry had been included); (2) because the same basic property of the centerline has been measured by several similar variables, exaggerating the importance of the corresponding eigenvector (for example, several measurements of meander wavelength were included in the database); and (3) because a common factor may be present in several measured variables (average channel width was used to normalize several variables). For these reasons, the discussion of the retained eigen-

vectors does not emphasize their relative importance and no tests of significance were conducted. However, redundant variables were eliminated during the analyses to minimize problem (2), as is discussed below.

The basic data gathered from meandering streams can be combined into a wide variety of derivative variables, and the resulting variables can be represented either linearly or as their logarithms. This wide latitude in defining variables presents a problem in determining which set best describes the natural pattern of meandering. Several guidelines were used. Most variables were entered as their original linear, or arithmetic values. However, variables defined as ratios, such as measures of sinuosity, were generally entered as their logarithms because of the multiplicative variance associated with ratios. Logarithmically-transformed variables are indicated in tables with an asterisk. Different sets of variables resulted in different numbers of eigenvalues greater than unity. Some of the associated eigenvectors may, however, represent covariant response of several variables to a single source of signal noise or they may result from non-linear relationships between variables that cannot be represented as a single linear component. One technique of judging the significance of eigenvectors is to apply the analysis to streams generated by the three-parameter DPM. Ideally, only three significant eigenvectors should result, and eigenvectors not strongly correlated with one of the three defining parameters are suspect.

Two types of FA were run on both the NAT and DPM streams. In the first, the 30–50 percentile and 60–90 percentile half-meander variables, as well as the other variables, were entered as originally calculated, or as "raw" data (except for the logarithmic transformation of some variables discussed above). In the second, some of the raw variables were replaced by "ratio" variables. In particular, the 30–50 percentile half-meander statistics were replaced with their ratios with the 60–90 percentile statistics; for example, λ_{hs} was replaced by the ratio $\lambda_{h\ell}/\lambda_{hs}$. These ratio variables are indicated by replacing the s subscript with an r. In addition, other pairs of variables measure similar meander characteristics at different scales and were included as ratios, as shown in Table 4a.

These ratio variables are indicated by the original variable notation with an added r in the subscript. The ratio variables allow a more direct comparison and contrast between properties of the longer and shorter half-meanders of a stream.

Elimination of redundant variables. The 44 measured variables (or their ratio equiva-

TABLE 4

Replacement and eliminated variables (see text).

(a)

Original	Replacement
$\lambda_{\{av\}}$	$\lambda_P/\lambda_{\{av\}}$
λ_{50}	$\lambda_{90}/\lambda_{50}$
λ_ξ	$\lambda_\theta/\lambda_\xi$
d_ξ	d_θ/d_ξ
e'_ξ	e'_θ/e'_ξ

(b)

Retained	Eliminated
$\xi_{\{sd\}}$	$\lvert\xi\rvert_{\{av\}}$ $\lvert\xi\rvert_{\{sd\}}$ $\lvert\xi\rvert_{h\{av\}\ell}$ $\lvert\xi\rvert_{h\{sd\}l}$ $\lvert\xi\rvert_{w\{av\}}$ $\lvert\xi\rvert_{R\{av\}}$
$\xi_{\{kr\}}$	$\lvert\xi\rvert_{\{sk\}}$ $\lvert\xi\rvert_{\{kr\}}$
μ^*_T	μ^*_R
$\lambda_{h\{av\}}$	λ_{90}
μ^*_H	$\mu^*_{h\ell}$ $\lvert\xi\rvert_{h\lambda\ell}$

(c)

Retained	Eliminated
$\lvert\xi\rvert^*_{h\{av\}r}$	$\lvert\xi\rvert^*_{h\{sd\}r}$ $\lvert\xi\rvert^*_{h\lambda r}$
d_θ	λ^*_{cr}
$\mathscr{A}_{h1l}$	$\mathscr{A}_{h2r}$

(d)

Retained	Eliminated
$\xi_{\{sd\}}$	$\lvert\xi\rvert_{h\{av\}s}$ $\lvert\xi\rvert_{h\{sd\}s}$
μ^*_{hs}	$\lvert\xi\rvert_{h\lambda s}$
d_ξ	$k_{\{cv\}}$
λ_ξ	$\lambda_{\{av\}}$

lents) are mathematically unique, but many of them are very highly intercorrelated when measured on natural or simulated meandering streams. It is desirable to eliminate redundancy within the FA variables for three reasons: (1) fewer variables are easier to interpret conceptually and to manipulate mathematically; (2) nearly linearly-dependent variables produce nearly singular matrices and unreliable FA results; and (3) inclusion of multiple, strongly intercorrelated variables result in factors strongly weighted on the intercorrelated variables that distorts their relative importance in stream meandering.

Redundant variables were identified by their pairwise correlations when applied to the sample of NAT or DPM streams. Redundancy was arbitrarily defined as pairwise correlations greater than 0.9 (or less than −0.9) within both the NAT and the DPM stream datasets. In general the variable that is conceptually most simple or most easily measured has been retained for each set of intercorrelated variables Twelve variables were eliminated from both the raw and ratio variable set, shown in Table 4b. In addition, an additional four variables were eliminated from the ratio variable set (Table 4c). Finally, four variables were also eliminated from the raw variable set (Table 4d).

Thus the redundancy analysis reduced the list of variables to 27 for the raw variable set and 28 for the ratio set. As a check, the analyses reported below using the reduced variable sets were also performed with the full variables in order to verify that discarding the redundant variables did not materially affect the interpretation of the FA or the power of the variable set to discriminate between NAT, DPM and HKM streams in the discriminant analysis discussed below.

Analysis of disturbed periodic streams. Eighty-three 50-wavelength streams were simulated using the DPM with the parameters of wavelength, damping, and error being varied through a reasonable range. The reduced variable set was measured on these streams and analyzed by FA using both the raw and ratio variables. The SPSS statistical package was used (Norusis, 1986); factors are extracted using the principal components method followed by varimax rotation. The analysis using the raw variables resulted in the direction-based autoregressive variables (which correspond the the wavelength, damping and error parameters used in creating the streams) not being well

TABLE 5

Normalized factor matrix and factor eigenvalues of 83 disturbed periodic model streams using ratio variables.

Variable	Factor					
	1	2	3	4	5	6
λ_θ	0.06	0.95	−0.06	−0.05	0.14	0.02
d_θ	0.96	−0.10	0.04	0.02	0.11	−0.11
e'_θ	0.77	−0.28	0.46	0.04	0.13	−0.20
$d^*_{\xi r}$	0.92	–	–	–	–	–
$e'^*_{\xi r}$	0.94	–	–	–	–	–
μ^*_T	–	–	0.71	–	–	–
μ^*_W	0.60	–	0.73	–	–	–
μ^*_H	–	–	0.86	–	–	–
μ^*_V	–	–	–	–	0.77	–
λ_P	–	0.90	–	–	–	–
$\lambda^*_{\{av\}r}$	0.88	–	–	–	–	–
$k_{\{cv\}}$	–	0.87	–	–	–	–
$\xi_{\{sd\}}$	–	−0.64	0.64	–	–	–
$\xi_{\{kr\}}$	–	0.60	–	–	–	–
$\lambda_{h\{av\}}$	−0.67	0.68	–	–	–	–
$\lambda_{h\{sd\}}$	–	0.90	–	–	–	–
$\lambda_{h\{sk\}}$	0.86	–	–	–	–	–
$\lambda_{h\{kr\}}$	–	–	–	–	0.86	–
μ^*_{hr}	–	–	0.88	–	–	–
$\lvert\xi\rvert^*_{h\{av\}r}$	–	–	–	–	–	0.72
$R^*_{\xi h\ell}$	0.76	–	–	–	–	–
$R^*_{\xi hr}$	0.86	–	–	–	–	–
$\mathscr{A}_{h1\ell}$	–	–	–	0.94	–	–
$\mathscr{A}_{h1r}$	–	–	–	0.81	–	–
$\mathscr{A}_{h2\ell}$	–	–	–	0.77	–	–
λ^*_{50r}	0.94	–	–	–	–	–
R^*_m	–	−0.60	–	–	–	–
R_t	–	–	–	–	–	–
Eigenvalue	9.5	5.5	3.1	2.3	2.0	1.2
% Variance	33.8	19.8	11.0	8.1	7.0	4.3

Only loadings greater than 0.6 are shown except for those involving model parameters. Variables marked with an * were logarithmically transformed.

separated into three factors with high eigenvalues. However, the analysis using the ratio variables successfully resolved the three model DPM variables (λ_θ, d_θ, and e'_θ) into the three factors with the highest eigenvalues. Table 5 presents the rotated factor matrix and percent variance explained for the six factors with eigenvalues greater than unity for the ratio variable FA. Because small factor loadings represent unimportant variables in each factor, only normalized factor loadings with absolute values greater than 0.6 are shown in the table (except that the DPM model parameters λ_θ, d_θ, and e'_θ are shown for each factor). The first two factors have strong loadings on the DPM model parameters, and the third a modest loading on e'_θ (however, note that the three DPM parameters are *not* represented in a single factor each with high loading). The last three factors have negligible loadings on the DPM model parameters and therefore can be regarded as "spurious", at least for the DPM streams. One of these factors is primarily weighted on the kurtosis variable $\lambda_{h\{sk\}}$. Another factor includes most of the variance of the asymmetry variables. The DPM model includes no inherent asymmetry. The high eigenvalues of these and the other spurious factors is due to the large random variability of the associated variables plus the covariant response of the variables. Therefore, when applying the FA to natural streams, factors explaining less than 8 percent of total variance will be viewed with suspicion, particularly if they are weighted on the same higher moment and asymmetry variables as in the DPM analysis. Thus factors explaining less than 8 percent of total variance might by *statistically* significant, but may not be *physically* significant for the meandering streams.

The three significant rotated factors can be interpreted as follows:

Factor 1, planform irregularity: Streams with high positive scores for this factor have a combination of high damping and high error, or perturbation, that is, they are irregular. Simulated streams scoring highly on this factor are visually highly irregular in planform at all scales, including pronounced wandering that is larger than the model wavelength (λ_θ) and many short-length, low-amplitude half-meanders interspersed with half-meanders near the model wavelength. By contrast, streams with high negative scores are slightly-irregular sine-generated curves having little planform wandering and few short half-meanders. The wide range of half-meander lengths (large $\lambda_{90}/\lambda_{50}$ values), the high curvature ratios in half-meanders, and the strong representation of high frequencies in the spectrum (high values of $\lambda_P/\lambda_{\{av\}}$ and $\lambda_\theta/\lambda_\xi$) in streams with positive scores are consistent with this interpretation. Such streams also tend to have high whole-meander and residual sinuosities. The irregularity primarily occurs at large rather than small spatial scales, as indicated by high positive weighting on $d^*_{\xi r}$ and $e'^*_{\xi r}$.

Factor 2, dominant wavelength: High scores on this factor are associated with long wavelength half-meanders relative to stream width. Thus the wavelengths λ_P, $\lambda\theta$, λ_{90}, and $\lambda_{h\{av\}}$ (measured in width-equivalents) are large, but the meandering is geometrically similar to streams with shorter characteristic wavelength (negative scores on this factor). Accordingly curvature variance is small but variance of half-meander length is large.

Factor 3, Amplitude of broad-scale meandering: This factor is moderately loaded on the disturbance parameter, e'_θ, and strongly loaded on variables related to high sinuosity of the longer half-meanders. Visually, streams with high scores on this factor have high-amplitude meandering, whereas negative scores are associated with streams that lack a well-defined wavelength of meandering although they are somewhat wandering at the broad scale.

Analysis of natural streams: Our a priori expectations were that at least three factors or dimensions would be needed to characterize natural streams. One of these would be associated with variations in the width-normalized wavelength of meandering, either due to natural

causes (such as variations among streams in width-depth ratio, friction factor, gradient, and variability of discharge) or due to "errors" introduced by map-making, digitizing, and differences between streams of the relative frequency of discharge at the time of aerial photography. The second expected factor would be variations between streams in amplitude of meandering, which would be reflected in average curvatures and half-meander sinuosities. One or more factors should be associated with the degree of regularity versus irregularity in the meandering pattern. Large (long) irregularities in pattern would be associated with wanderings of the valley axis (that is, with large total, whole-meander, and valley sinuosities), and small (short) irregularities would be associated with large variabilities in curvature and a presence of a large number of small half-meanders. Finally, natural streams might differ amongst themselves in regard to the degree of asymmetry of meanders.

Table 6 presents the results of FA applied to the 57 segments of natural (NAT) streams using the ratio variables. The resulting factors resemble those for the DPM FA, with some differences:

Factor 1, spread of meander wavelengths: Positive scores on this factor are related to the presence of primarily long and regular half-meanders interspersed with low amplitude half-meanders of considerably shorter wavelength, giving a bimodal distribution of half-meander lengths. Visually, streams with positive scores on this factor would be characterized as having a regular meandering pattern dominated by a well-defined long-wavelength component with modest short-wavelength irregularity between larger meanders. Streams with negative scores on this factor have a shorter characteristic wavelength of meandering with a narrow range of half-meander sizes which are very sinuous with large mean curvature. High loadings on both width-normalized and ratio variables suggests that errors in measuring effective channel width (from measurement errors or different flow frequencies at the times of aerial photography) are small compared to other, systematic variations of meander properties with channel width.

TABLE 6

Normalized factor matrix and factor eigenvalues for 57 freely-meandering natural streams, using ratio variables.

Variable	Factor					
	1	2	3	4	5	6
λ_θ	0.74	–	–	–	–	–
d_θ	0.70	–	–	–	–	–
e'_θ	–	–	–	0.89	–	–
$d^*_{\xi r}$	–	−0.69	–	–	–	–
$e'^*_{\xi r}$	–	−0.62	–	–	–	–
μ^*_T	–	–	–	0.78	–	–
μ^*_W	–	–	–	–	–	–
μ^*_H	–	0.89	–	–	–	–
μ^*_V	–	–	–	–	–	–
λ_P	0.68	–	–	–	–	–
$\lambda^*_{\{av\}r}$	0.69	–	–	–	–	–
$k_{\{cv\}}$	0.78	–	–	–	–	–
$\xi_{\{sd\}}$	−0.67	–	–	–	–	–
$\xi_{\{kr\}}$	–	−0.64	–	–	–	–
$\lambda_{h\{av\}}$	–	–	0.73	–	–	–
$\lambda_{h\{sd\}}$	0.77	–	–	–	–	–
$\lambda_{h\{sk\}}$	–	–	–	–	–	0.90
$\lambda_{h\{kr\}}$	–	–	–	–	–	0.94
μ^*_{hr}	–	0.87	–	–	–	–
$\lvert\xi\rvert^*_{h\{av\}r}$	0.88	–	–	–	–	–
R^*_{ghl}	–	–	0.70	–	–	–
R^*_{ghr}	0.91	–	–	–	–	–
$\mathscr{A}_{h1\ell}$	–	–	–	–	0.93	–
$\mathscr{A}_{h1r}$	–	–	–	–	0.79	–
$\mathscr{A}_{h2\ell}$	–	–	–	–	0.70	–
λ^*_{50r}	0.88	–	–	–	–	–
R^*_m	−0.86	–	–	–	–	–
R_t	–	–	−0.89	–	–	–
Eigenvalue	10.9	5.5	2.7	2.1	1.5	1.3
% Variance	39.0	19.6	9.7	7.3	5.3	4.5

Only loadings greater than 0.6 are shown. Variables with an * were logarithmically transformed.

Factor 2, short-wavelength irregularity: This factor is primarily related to the relative contributions of long and short wavelengths to the stream sinuosity. Rivers with high scores on this factor have smooth and sinuous longer half-meanders alternating with modest-amplitude short half-meanders. Streams with negative scores on this factor either are irregular

with short, low-amplitude half-meanders and little evidence of regular, long-wavelength meandering or have long-wavelength meandering broken up by superimposed small meandering; both sinuosities and average curvatures of half-meanders are small. Note that such *superimposed* short-wavelength meandering disrupting a longer wavelength meandering is distinct from the situation of streams weighted positively on Factor 1 in which the short wavelength half-meanders are *interspersed* with the longer half-meanders without interference. Cases of superimposed short meanders could be due to local variations in bank erodibility, temporal decrease in effective discharge causing breakup of long meanders into shorter, or due to effects of short-wavelength alternate bars on bank erosion. These influences on meander form are considered further in the Discussion.

Factor 3, wavelength of half-meanders: Streams scoring positively on this factor tend to consist primarily of long, gently-curving half-meanders with little tendency for them to be broken by short irregularities. Negatively-scoring streams are dominated by short, sinuous, strongly curving half-meanders often alternating with nearly straight channel sections.

Factor 4, long-wavelength irregularity: This factor is correlated almost entirely with total, whole-meander, and valley sinuosity as well as the disturbance parameter, e'_θ. Visually streams with high scores on this factor are dominated by low amplitude short wavelength meandering superimposed onto high-amplitude, long-wavelength wanderings, generating a complicated pattern, whereas streams with negative scores have regular, "sine-generated" meanders of moderate to low amplitude and a narrow range of wavelengths. Streams with high scores on this factor may derive their large-scale wandering from geologic controls. Alteratively, streams with negative scores may represent youthful meandering and positive scores may correspond to an old meandering pattern, similar to the temporal sequence in HKM streams that initially evolve from a straight stream into regular, sine-generated meanders (negative scores on this factor) and eventually grow into more complicated forms with large-scale wandering (positive scores) as meander amplitude becomes large enough for cutoffs to occur (Howard and Knutson, 1984). Streams with small wavelength meandering superimposed on a larger meandering also have positive scores on this factor (as well as negative scores on Factor 2).

The fifth and sixth factors are nearly identical in the highly loaded variables to factors four to six for the DPM streams and explain less than 8 percent of total variance. That is, they are primarily loaded by variables measuring the higher statistical moments and by the asymmetry variables. Therefore, they probably represent statistical noise rather than significant form variations among natural streams. The major difference is that the half-meander pathlength skewness, $\lambda_{h\{sk\}}$, is strongly correlated with the kurtosis, $\lambda_{h\{kr\}}$, in natural streams, whereas in the DPM streams the skewness is independent of the kurtosis, but is instead strongly correlated with Factor 1. Also, although the asymmetry parameters in NAT streams are not strongly correlated with the factors listed above, the mean value of asymmetry is significantly less than zero (upstream skewing).

A factor analysis was also performed using the raw variables, producing three main factors which, however, differed rather strongly in the distribution of variable loadings from the ratio variables FA. The difference in variable loadings between analyses using raw and ratio variables indicates that the factors are not strongly unique. That is, addition, removal, or transformation of a few variables can strongly affect the patterns of variable loadings in the factors. Also symptomatic of a lack of uniqueness is the lack of strong pairwise correspondence between the leading DPM and NAT factors in terms of the mix of strongly loaded variables. Rather, each of the first four NAT

factors combines aspects of two or three of the leading three DPM factors. A broader range of samples of natural streams might help to constrain the factors. For example, few streams of very low sinuosity were included, with the result that no single factor emerges that is primarily related to this variable.

In a similar vein, although factor 5, loaded on asymmetry variables, conforms to prior expectations, the factors that resulted using either raw or ratio variables did not separate cleanly into the expected dimensions related to wavelength, amplitude and pattern regularity. Only further sampling, and possibly inclusion of additional or altered variables, will determine whether the a priori expectations overlooked strong interactions between these expected dimensions.

O'Neill (1987) performed a similar factor analysis on 75 freely-meandering reaches from 51 streams, including several of the same rivers included in the present sample. His variables, although defined differently, measure most of the same characteristics of meandering. His results correspond most closely to our analysis using unratioed variables.

Discriminant analysis

The morphometric variables introduced in this paper permit statistical testing of the degree of similarity between natural meandering streams and theoretical models of stream meandering, thereby evaluating the adequacy of the models to emulate the statistical properties of natural meanders. Discriminant analysis is a technique by which $K-1$ (or fewer) optimal linear functions of the input variables are derived which best separate, or discriminate between samples from K known populations with the assumption that each population is multivariate normal (Davis, 1986; Kleinbaum and Kupper, 1978).

Three populations were utilized in this study, the first being the sample of 57 natural (NAT) streams. The second population was the DPM streams discussed earlier. In addition to the 83 original streams generated by the DPM, a derivative sample was created from the original streams by filtering the x and y sample coordinates with a three-point, uniform-weight moving average followed by re-sampling at a one width-equivalent spacing. This second sample was created because many natural streams appear to have little high-frequency noise as compared to the DPM streams, perhaps due both to generalization of the stream pattern in map-making and to the smoothing effects of flood discharges upon channel form. The total DPM sample was 165 streams; one filtered stream was omitted because the filtering process created a closed half-meander that caused numerical overflow.

The third sample was composed of 227 streams generated by HKM simulation models under various model assumptions and parameter values. Most simulations were based upon the theoretical model of Ikeda, et al. (1981) which proposes that the rate of bank erosion is proportional to the near-bank velocity perturbation, u, given by:

$$u=\frac{U-V}{V} \tag{29}$$

where U is the depth-averaged near-bank velocity and V is the average velocity for the entire channel. Ikeda et al. (1981) propose that the velocity perturbation is a function of the channel curvature and the flow parameters:

$$\frac{\partial u}{\partial s}+\alpha u=K\left(\frac{\partial \xi}{\partial s}+\frac{\alpha}{2}\left(F^2X^3+A\right)\xi\right) \tag{30}$$

where s is the downstream distance along the centerline, F is the flow Froude number, A relates the cross-channel bed slope to channel curvature, and the remaining parameters are given by:

$$\alpha=2Xf/D \tag{31}$$

$$X=\mu_{\mathrm{T}}^{-1/3} \tag{32}$$

$$K=\tfrac{1}{2}WVX \tag{33}$$

In these formulas the channel width is W and the average depth is D, and f is a friction factor expressed as the ratio of the square of the shear velocity to the average velocity. Since K is independent of position along the channel, the spatial distribution of erosion rates is primarily determined by the parameters α and A (the product F^2X^3 is much smaller than A for most streams). As shown by Howard and Knutson (1984) these parameters jointly determine the dominant wavelength of meandering. Equation (29) can be solved either by successive iterations utilizing a convolution integral approach as indicated by Howard and Knutson (1984) or by an autoregressive approach similar to that used to represent eq. (7) by eqs. (8–11). Both types of approaches were used in the sample streams, with equivalent results.

In addition to varying the two model parameters α and A, several other modifications were made to the model to test their effect upon realism of modeling:

(1) Spatially variable bank resistance was incorporated in some simulations by randomly assigning bank resistances from a lognormal distribution with a mean of unity and a pre-assigned variance. Because bank erodibility is likely to vary as the channel migrates across the floodplain, the resistance was randomly reassigned whenever the channel migrated through a distance equal to one channel width. When new reassignments were made or new nodes were added, the new resistance was made equal to a lognormal perturbation from the average of the resistances of the adjacent upstream and downstream nodes.

(2) Temporal variations in discharge affect the process of bank erosion both by changes in average shear stress as well as by variations in flow momentum, which affects the parameter α and thus the dominant meander wavelength. Temporal flow variations were modeled in some of the simulated runs by assigning the discharge for each iteration from a lognormal distribution of a pre-assigned variance and mean of unity. Based upon the variation of discharge and using typical equations of hydraulic geometry, the parameters α and K were appropriately varied.

(3) For a few simulations an additional term, $\gamma(\partial^2\xi/\partial s^2)$, was experimentally added to eq. (29) with differing values of γ to test the effect of a higher-order curvature correction.

(4) Odgaard (1986) has proposed a flow model for meanders that is similar in broad outline but differing in detail from the Ikeda et al. model. The Odgaard model was substituted for the Ikeda et al. model for several simulations.

(5) In some simulations the bank erosion rate law was varied from a linear dependence upon u. A more general rate law is assumed:

$$E = C_r(u-\delta)^a d^b \tag{34}$$

where E is the bank erosion rate, C_r is a rate constant, δ is a constant with the values zero or unity, d is the near-bank depth, and a and b are exponents. The parameters were individually varied in several simulations from their nominal values of $\delta=0$, $a=1$ and $b=0$ to the values $\delta=1$, $a=0.5$ or 2, and $b=-0.5$, 0.5, or 1. Since C_r affects only the overall rate of erosion and not the local pattern, it was not varied. In the nominal simulation model the velocity perturbation u is taken to be the largest of the two values on the opposing banks, and the bank erosion is directed perpendicular to that bank. Additionally in some simulations u is assumed to be the difference between the values on opposite banks.

(6) Most of the simulations were input into the database both in raw form as output as well as in a version in which a uniform 3-point moving average was applied to remove high-frequency noise. This procedure was the same as applied to the DPM streams.

The SPSS DISCRIMINANT program using the RAO step-wise method and default parameters was used for the analysis (Norusis, 1986). The raw (non-ratio) variables were utilized. Figure 8 shows the scores of the three samples of streams (NAT, HKM, and DPM) plotted

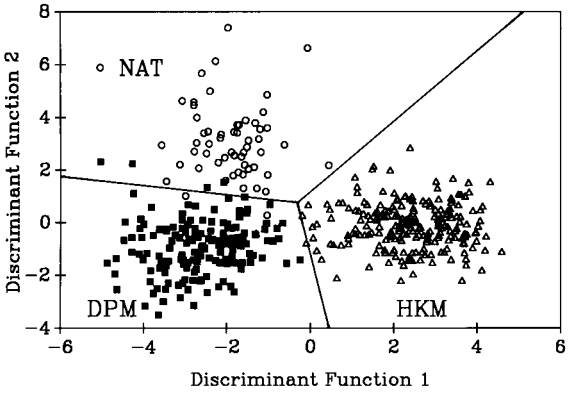

Fig. 8. Discriminant function scores for NAT (○), DPM (■), and HKM (△) streams, showing nearly perfect discrimination between populations. Classification fences are also shown.

versus the two discriminant functions (DF). As is clear from this plot, the three samples have minimal overlap. That is, the statistical variables defined here when taken together are clearly capable of discriminating natural streams from two models of meandering, despite the apparent visual similarity between the three types of streams (Fig. 1).

Table 7 shows the correlations between the two DF's and the morphometric variables. These correlation coefficients indicate the relative contribution of the variables to the discriminant function. NAT streams are distinguished from DPM streams primarily by high scores on DF 2. This implies that NAT streams should by characterized by large positive values of those variables in Table 7 that have strong, positive correlations with DF 2. Thus, compared to DPM streams, natural streams have higher irregularity of planform at large scales and numerous, low-sinuosity short half-meanders (larger values of $R^*_{\xi hl}$, $R^*_{\xi hr}$, μ^*_V, $e'^*_{\xi r}$, d_θ, and $d^*_{\xi r}$), as well as a wider range of half-meander sizes (a less well-defined frequency of meandering, as indicated by high $\lambda^*_{50_r}$ and $\lambda_{h\{sk\}}$). This DF correlates highly with most of the strongly-loaded variables of factors 1 and 5 of the DPM FA (Table 5), but it is not as simply related to factors in the NAT FA (Table 6).

Natural streams also tend to have similar

TABLE 7

Correlations between variables and the two discriminant functions.

Variable	Function 1	Function 2
μ^*_H	0.60	−0.03
μ^*_T	0.46	0.24
$\mathscr{A}_{hl\ell}$	−0.43	−0.05
μ^*_W	0.42	0.13
$\mathscr{A}_{h2\ell}$	−0.40	−0.08
$\mathscr{A}_{hlr}$	−0.37	−0.10
$\mu_{hr}{}^*$	0.36	−0.07
$\lvert\xi\rvert^*_{h\{av\}r}$	−0.35	0.17
$\lambda_{h\{sk\}}$	0.10	0.57
$R^*_{\xi hr}$	−0.13	0.52
$\lambda^*_{50_r}$	0.03	0.51
$R^*_{\xi h\ell}$	−0.01	0.48
μ^*_V	−0.19	0.44
$e'^*_{\xi r}$	0.23	0.42
d_θ	−0.27	0.41
$d^*_{\xi r}$	0.00	0.30

Only variables correlating with at least one discriminant function at 0.3 or greater are listed. Ratio variables were used in this analysis. Variables with an * were logarithmically transformed.

differences from HKM streams (high scores on DF 2), but in addition have low weighting on DF 1, implying that natural streams have less sinuous half-meanders (smaller values of μ^*_H), particularly for the longer wavelengths (low μ^*_{hr} and $\lvert\xi\rvert_{h\{av\}r}$), smaller overall sinuosity (μ^*_T), and lesser upstream skewing of half-meanders (negative weighting on $\mathscr{A}_{hl\ell}$ and $\mathscr{A}_{h2\ell}$) than HKM streams.

Discussion

The minimal overlap between NAT, DPM, and HKM streams in the discriminant analysis indicates that the two models fail to replicate aspects of natural meandering. In general, even with variable bank resistance in the HKM models and the disturbance parameter in the DPM model, the simulated streams show too great a regularity in meander sizes and shapes, and in the case of HKM simulations, meanders of exaggerated sinuosity. Several features of natural meandering are not incorporated in the models:

(1) Meander characteristics of natural streams change from each to reach due to variations in bed and bank sediment characteristics, valley gradient, and flow characteristics. This introduces downstream variations that increase the variance of shape and size parameters. As discussed above, the autoregressive parameters C_1 and C_2 were used as a check on downstream changes, but some types of nonstationarity may not have been detected. However, this factor is unlikely to be an important effect in all streams, and thus cannot account for the universal discrimination.

(2) Some natural meandering streams appear to have short meanders superimposed upon larger meanders, often generating the compound or cumuliform meander forms noted by Brice (1974b) and Hickin (1974). Neither the HKM or DPM model incorporates more than one dominant wavelength of meandering. The development of cumuliform meanders can account for the statistical differences between natural and model streams due to the greater range of bend sizes and a enhanced tendency for cutoffs to develop due to lateral bends growing upon longer bends. Superimposition of wavelengths can occur by at least two mechanisms. One is an historical decrease of dominant wavelength, such as would result from a long-term decrease in flood peaks, so that short, new meanders develop on older, larger meanders. This may have occurred on a few of the natural streams, but is unlikely to be the dominant reason for discrepancies between the models and natural streams.

A more fundamental cause of multiple wavelengths is the simultaneous action of two distinct processes creating meandering in streams. One is the secondary circulation created by stream curvature which is incorporated in the theory of Ikeda et al. (1981) and the HKM model. The second is the flow and bed resonances resulting in fixed or migrating alternate bars (Engelund and Skovgaard, 1973; Parker, 1976; Fredsoe, 1978). Experiments by Whiting and Dietrich (1989) indicate that several fixed alternate bars may occur in a single long, high amplitude meander bend and may influence bank erosion rates such that the bends develop the cumuliform shapes mentioned above. Recent theories of flow and bed topography in meanders (e.g. Johannesson and Parker, 1989; Parker and Johannesson, 1989) account for time-averaged effects of alternate bars, as a result of including additional terms in the flow equations as well as an erodible bed with sediment continuity. Furthermore, the more general models of Nelson and Smith (1989a,b) and Shimizu and Itakura (1989) account for alternate bar migration. To date these new models have not been implemented to generate long simulated streams.

(3) Bank erodibility has systematic as well as random variability. In particular, bank erosion is hindered or stopped by impingement or natural levees and by exposure of clay plugs from old oxbow lakes (Fisk, 1947; Ikeda, 1989). It is uncertain whether these effects are sufficiently widespread or regular to affect meander patterns in a manner accordant with the discrepancies between natural and model streams.

Although the variables introduced in this paper are able to readily discriminate between natural streams and current theoretical models for sufficiently long samples of stream, it is important to emphasize that the theoretical models offer good first-order approximations to natural meandering. In particular, the HKM model gives reasonable estimates of spatial patterns of expected bank erosion (Howard and Knutson, 1984) and the model can be extended and modified to examine historical patterns of floodplain sedimentation and fluvial stratigraphy.

The variable loadings in the factor analyses indicate that the variables separate into groups characterizing different spatial scales of meandering. Meandering at the broadest scale is characterized by d_θ, e'_θ, and μ_V. The shape, size, and dominance of the longer (60–90 percentile of length) half-meanders is measured by λ_{90}

and the 60–90 percentile half-meander statistics. If the meandering is simple in pattern then the broad-scale wavelengths, λ_P and λ_θ, will be close to λ_{90}, but if there is broad-scale irregularity or if large half-meanders have been broken up by superimposed small meanders, then λ_{90} will be much smaller than λ_P and λ_θ. The variables λ_{50}, $\lambda_{\{av\}}$, λ_ξ, d_ξ, e'_ξ, $\xi_{\{sd\}}$, and the 30–50 percentile half-meander statistics primarily characterize the shorter half-meanders. If meandering occurs in a narrow range of wavelengths then λ_{90} will be close to λ_{50} and the 60–90 and 30–50 percentile statistics will be similar, but if a wide range of wavelengths occurs, these statistics will be widely divergent in value. A wide range of meandering wavelengths is associated with short-wavelength, low-amplitude half-meanders interspersed with longer ones.

In addition to the redundant variables that were eliminated prior to the principal component and discriminant analyses, several other variables are probably unimportant, in the sense that they are not strongly correlated with other variables or they appear to be statistical "noise", and in addition, they are not useful in distinguishing between NAT, DPM, and HKM streams. The variables expressing curvature and half-meander kurtosis ($\xi_{\{kr\}}$ and $\lambda_{h\{kr\}}$) are unimportant in this sense. The low significance of higher statistical moments (skewness and kurtosis) results because of their high variability (Table 3) and probably also because of the lack of natural processes related to these variables, with the exception of half-meander length skewness ($\lambda_{h\{sk\}}$), which is important in discriminating NAT from DPM streams. The half-meander asymmetry variables ($\mathscr{A}_{h1\ell}$, $\mathscr{A}_{h1r}$ and $\mathscr{A}_{h2\ell}$) are uncorrelated with other variables within NAT, DPM, or HKM streams, but they are important in distinguishing between these types of streams (DPM streams are symmetrical, natural streams skewed slightly upstream, and HKM streams strongly skewed upstream). Of the asymmetry measures, $\mathscr{A}_{h1\ell}$ is the best discriminator.

The factor analysis suggests even fewer (3 to 5) natural dimensions to meandering. However, since these components are weighted sums of more than 25 measured variables, they are only partially characterized by any single variable. However, for particular purposes a reduced set of variables could be used. For example, the important factors identified for natural streams are well represented by one to three leading variables, as summarized below:

Factor 1, spread of meander wavelength: $R^*_{\xi hr}$, λ^*_{50r} and $|\xi|^*_{h\{av\}r}$.
Factor 2, short-wavelength irregularity: μ^*_H and μ^*_{hr}.
Factor 3, wavelength of half-meanders: R_t and $\lambda_{h\{av\}}$.
Factor 4, long-wavelength irregularity: e'_θ and μ^*_T.

There are probably additional variables that would either better characterize the natural dimensions of meandering or that would measure additional and useful aspects of meander geometry not considered in this study. In particular, one or more variables could characterize *sequencing* of half-meander characteristics, measuring, for example, whether a long half-meander is more likely to be followed by another long bend or a much shorter one.

The statistical techniques introduced in this paper could be extended in several ways. The database of streams could be enlarged to include alluvial streams that are confined between narrow valley walls. As pointed out by Allen (1982) and Howard and Knutson (1984), lateral confinement of meanders distorts their shapes in characteristic ways (primarily by development of strong negative asymmetry and a narrow range of half-meander sizes) that should give distinctive variable values. Similarly, measurements can be extended to meanders incised in bedrock. O'Neill (1987) has already sampled such streams and find that they differ in statistical characteristics from non-incised streams.

Another extension of the present techniques would be to include environmental, historical, and within-channel measurements in the database. Environmental variables would include discharge and sediment load characteristics. Within-channel data could include channel bank and bed sediment variables, width-depth ratios, channel gradient, and bank vegetation characteristics. Old maps and air photos can be used to estimate average bank migration rates. This data can be used to provide insight into how such variables are related to meander geometry. The work of Hickin and Nanson (1975, 1984) and Nanson and Hickin (1986) are pioneering efforts in this direction, relating migration rates to bend curvature and sediment and flow characteristics.

Finally, morphometric variables similar to those used in the present study could be applied to other quasi-periodic natural phenomena, such as ripple and dune profiles, water waves, and sedimentary coastlines characterized by a regular cuspate planform. For example, use of multivariate form parameters might prove useful in distinguishing between bedforms formed in different environments (eolian, fluvial, continental shelf, etc.) and varying flow conditions (flow depth, Froude number, unidirectional versus oscillatory, etc.)

Acknowledgements

The manuscript was substantially improved as a result of comments by John Porter, Luna Leopold, and two anonymous reviewers. The study also benefited from discussions with Mike O'Neill.

Appendix. Notation

Part I. Variable definitions

Variable	Defining equation[a]	Description
λ_θ	(9–11)	Autoregressive direction wavelength
d_θ	(9–11)	Autoregressive direction damping
e'_θ	(12)	Autoregressive direction disturbance
λ_ξ	(9–11)	Autoregressive curvature wavelength
d_ξ	(9–11)	Autoregressive curvature damping
e'_ξ	(12)	Autoregressive curvature disturbance
μ_T	(1)	Total sinuosity
μ_W	(3)	Full-meander sinuosity
μ_H	(4)	Half-meander sinuosity
μ_R	(5)	Residual sinuosity
μ_V	(5+)	Valley sinuosity
λ_P	(5+)	Spectral peak wavelength
$\lambda_{\{av\}}$	(6)	Average spectral wavelength
$k_{\{cv\}}$	(6+)	Coefficient of variation of spectral frequency
$\xi_{\{sd\}}$	(14+)	Standard deviation of curvature
$\xi_{\{kr\}}$	(17)	Kurtosis of curvature
$\lvert\xi\rvert_{\{av\}}$	(14+)	Average absolute curvature
$\lvert\xi\rvert_{\{sd\}}$	(14+)	Standard deviation of absolute curvature
$\lvert\xi\rvert_{\{sk\}}$	(15)	Skewness of absolute curvature
$\lvert\xi\rvert_{\{kr\}}$	(17)	Kurtosis of absolute curvature
$\lvert\xi\rvert_{W\{av\}}$	(19)	Average whole-meander absolute curvature
$\lvert\xi\rvert_{R\{av\}}$	(18)	Average half-meander absolute curvature
$\lambda_{h\{av\}}$	(19+)	Average half-meander wavelength
$\lambda_{h\{sd\}}$	(19+)	Standard deviation of half-meander wavelength
$\lambda_{h\{sk\}}$	(19+)	Skewness of half-meander wavelength
$\lambda_{h\{kr\}}$	(19+)	Kurtosis of half-meander wavelength
μ_h	(20)	Half-meander sinuosity
$\lvert\xi\rvert_{h\{av\}}$	(21)	Average half-meander absolute curvature
$\lvert\xi\rvert_{h\{sd\}}$	(21+)	Standard deviation of half-meander absolute curvature
$R_{\xi h}$	(22)	Average half-meander curvature ratio
$\lvert\xi\rvert_{h\lambda}$	(23)	Average length-normalized half-meander curvature
$\mathscr{A}_{h1}$	(24)	Average half-meander asymmetry index 1
$\mathscr{A}_{h2}$	(26)	Average half-meander asymmetry index 2
λ_{90}	(28+)	Ninetieth percentile half-meander wavelength
λ_{50}	(28+)	Median half-meander wavelength
R_m	(27)	Relative mid-size half-meander frequency
R_l	(28)	Relative small versus large half-meander frequency

Part II. Other notation in tables

s	Average value for 30–50 length percentile half-meanders (subscript)
ℓ	Average value for 60–90 length percentile half-meanders (subscript)
r	Variable redefined as its inverse ratio to another variable (subscript)
*	Logarithmically-transformed variable

[a]A plus sign after the equation number means that the variable is verbally defined in the text succeeding the equation.

References

Allen, J.R.L., 1982. Free meandering channels and lateral deposits. In: Sedimentary Structures: Their Character and Physical Basis, 2. Elsevier, New York, pp. 53–100.

Brice, J.C., 1974a. Meander pattern of the White River in Indiana: An analysis. In: M. Morisawa (Editor), Fluvial Geomorphology. State University of New York, Binghamton, pp. 178–200.

Brice, J.C., 1974b. Evolution of meander loops. Geol. Soc. Am. Bull., 85: 581–586.

Box, G.P. and Jenkins, G.M., 1976. Time Series Analysis: Forecasting and Control. Holden-Day, Oakland, 575 pp.

Carson, M.A. and Lapointe, M.F., 1983. The inherent asymmetry of river meander planform. J. Geol., 91: 41–55.

Chang, T.P. and Toebes, G.H., 1970. A statistical comparison of meander planforms in the Wabash Basin. Water Resour. Res., 6: 557–578.

Davies, T.R.H. and Tinker, C., 1984. Fundamental characteristics of stream meanders. Geol. Soc. Am. Bull., 95: 505–512.

Davis, J.C., 1986. Statistics and Data Analysis in Geology, 2nd ed. Wiley, New York, 646 pp.

Engelund, F. and O. Skovgaard, 1973. On the origin of meandering in alluvial streams. J. Fluid Mech., 57: 289–302.

Ferguson, R.I., 1973. Regular meander path models. Water Resour. Res., 9: 1079–1086.

Ferguson, R.I., 1975. Meander irregularity and wavelength estimation. J. Hydrol., 26: 315–333.

Ferguson, R.I., 1976. Disturbed periodic model for river meanders. Earth Surf. Proc., 1: 337–347.

Ferguson, R.I., 1979, River meanders: regular or random? In: N. Wrigley, (Editor), Statistical Applications in the Spatial Sciences. Pion, London, pp. 228–241.

Fisk, H.N., 1947. Fine grained alluvial deposits and their effects upon Mississippi River activity. Rep., Mississippi River Commission, Waterways Experiment Station, U.S. Army Corps of Engineers, Vicksburg, Miss., 40 pp.

Fredsoe, J., 1978. Meandering and braiding of rivers. J. Fluid Mech., 82: 609–624.

Hemberger, A.T., 1986. River Meander Morphometrics, MSc Thesis, University of Virginia, unpubl.

Hey, R.D., 1976. Geometry of river meanders. Nature, 262: 482–484.

Hey, R.D., 1984. Plan geometry of river meanders. In: River Meandering. Am. Soc. Civil Eng., New York, pp. 30–43.

Hickin, E.J., 1974, Development of meanders in natural river-channels. Am. J. Sci., 274: 414–442.

Hickin, E.J. and Nanson, G.C., 1975. The character of channel migration on the Beatton River, northeast British Columbia, Canada. Geol. Soc. Am. Bull., 86: 487–494.

Hickin, E.J. and Nanson, G.C., 1984. Lateral Migration of River Bends. J. Hydraul. Eng. Am. Soc. Civil Eng., 110: 1557–1567.

Hooke, J.M., 1984. Changes in river meanders: A review of techniques and results of analyses. Prog. Phys. Geogr., 8: 473–508.

Howard, A.D., 1983. Simulation model of meandering. In: River Meandering. Am. Soc. Civil Eng., New York, pp. 952–963.

Howard, A.D. and Knutson, T.R., 1984. Sufficient conditions for river meandering: A simulation approach. Water Resour. Res., 20: 1659–1667.

Ikeda, H., 1989. Sedimentary controls on channel migration and origin of point bars in sand-bedded meandering rivers. In: S. Ikeda and G. Parker, (Editors), River Meandering. Water Resources Monograph 12. Am. Geophys. Union, Washington, pp. 51–68.

Ikeda, S., Parker, G. and Sawai, K., 1981. Bend theory of river meanders. 1. Linear development. J. Fluid Mech., 112: 363–377.

Johannesson, H. and G. Parker, 1989. Linear theory of river meanders. In: S. Ikeda and G. Parker (Editors), River Meandering. Water Resources Monograph 12. Am. Geophys. Union, Washington, pp. 181–213.

Joreskog, K.G., Klovan, J.E. and R.A. Reyment, 1976. Geological Factor Analysis. Elsevier, Amsterdam, 178 pp.

Kleinbaum, D.G. and L.L. Kupper, 1978. Applied Regression Analysis and Other Multivariable Methods. Duxbury Press, North Scituate, Mass., 566 pp.

Lapointe, M.F. and Carson, M.A., 1986. Migration patterns of an asymmetric meandering river: The Rouge River, Quebec. Water Resour. Res., 22: 731–743.

Leopold, L.B. and Wolman, M.G., 1957, River channel patterns Braided, meandering, and straight, U.S. Geol. Surv. Prof. Pap., 282-B: 39–85.

Leopold, L.B. and Wolman, M.G., 1960. River meanders. Geol. Soc. Am. Bull., 71: 769–784.

Nanson, G.C., 1980. Regional trend to meander migration. J. Geol., 88: 100–108.

Nanson, G.C. and Hickin, E.J., 1986. A statistical analysis of bank erosion and channel migration in western Canada. Geol. Soc. Am. Bull., 97: 497–504.

Nelson, J.M. and Smith, J.D., 1989a. Flow in meandering channels with natural topography. In: S. Ikeda and G. Parker (Editors), River Meandering. Water Resources Monograph1, 12. Am. Geophys. Union, Washington, pp. 69–102.

Nelson, J.M. and Smith, J.D., 1989b. Evolution and stability of erodible channel beds. In: S. Ikeda and G. Parker (Editors), River Meandering. Water Resources Monograph, 12. Am. Geophys. Union, Washington, pp. 321–378.

Norusis, M.J., 1986. Advanced Statistics, SPSS/PC+, for

the IBM PC/XT/AT, SPSS Inc., Chicago.
O'Neill, M.P., 1987. Meandering Channel Patterns: Analysis and Interpretation, PhD Dissertation, State University of New York, Buffalo, 212 pp., unpublished.
O'Neill, M.P. and Abrahams, A.D., 1986. Objective identification of meanders and bends. J. Hydrol., 83: 337–353.
Odgaard, A.J., 1986. Meander-flow model 1; development. J. Hydraul. Eng., Am. Soc. Civil Eng., 112: 1117–1136.
Parker, G., 1976. On the cause and characteristic scales of meandering and braiding. J. Fluid Mech., 76: 457–480.
Parker, G. and Johannesson, H., 1989. Observations on several recent theories of resonance and overdeepening in meandering channels. In: S. Ikeda and G. Parker (Editors), River Meandering. Water Resources Monograph, 12. Am. Geophys. Union, Washington, pp. 379–415.
Preisendorfer, R.W., Zweirs, F.W. and Barnett, T.P., 1981. Foundations of Principal Component Selection Rules. Scripps Institution of Oceanography, University of California, SIO Reference Series 81-4, 192 pp.
Schumm, S.A., 1968. River adjustment to altered regimen: Murrumbidgee River and Paleochannels, Australia. U.S. Geol. Surv. Prof. Pap., 352-B.
Shimizu, Y. and T. Itakura, 1989. Calculation of bed variation in alluvial channels. J. Hydraul. Eng., 115: 367–384.
Speight, J.G., 1965. Meander spectra of the Angabunga River. J. Hydrol., 3: 1–15.
Speight, J.G., 1967. Spectral analysis of meanders of some Australasian rivers. In: J.N. Jennings and J.A. Mabbutt (Editors), Landform Studies from Australia and New Guinea. Cambridge University Press, Cambridge, pp. 48–63.
Stauffer, D.F., Garton, E.O. and Steinhorst, R.K., 1985. A comparison of principal components from real and random data. Ecology, 66: 1692–1698.
Thakur, T.R. and Scheidegger, A.E., 1968. A test for the statistical theory of meander formation. Water Resour. Res., 4: 317–329.
Thakur, T.R. and Scheidegger, A.E., 1970. Chain model of river meanders. J. Hydrol., 12: 25–47.
Whiting, P.J., and W.E. Dietrich, 1989. Multiple bars in highly sinuous flume bends: Implications for bank erosion and bed evolution EOS, 70: 329 (abstract).
Williams, G.P., 1986, River meanders and channel size. J. Hydrol., 88: 147–164.
Young, P., 1984. Recursive Estimation and Time-Series Analysis. Springer, Berlin, 300 pp.